Off-Line Sensing: Memorizing Interactions in Passive 3D-Printed Objects

Martin Schmitz, Martin Herbers, Niloofar Dezfuli, Sebastian Günther, Max Mühlhäuser
Technische Universität Darmstadt
Hochschulstraße 10, 64289 Darmstadt, Germany
{schmitz,herbers,dezfuli,guenther,max}@tk.tu-darmstadt.de

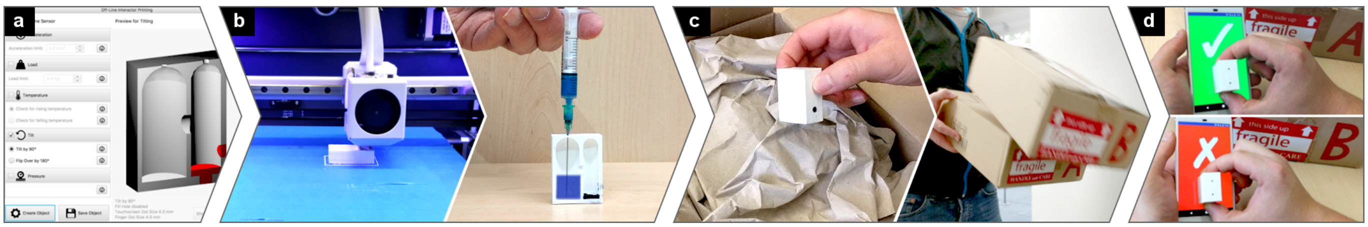

Figure 1. An off-line sensor may monitor whether a fragile parcel was improperly tilted: After the sender specifies the sensor in a design UI (a), two identical sensors are 3D-printed and filled with a conductive liquid (b). After placing each sensor into parcels A and B, both are shipped (c). The recipient checks whether the sensor was exposed to tilting by placing it on her capacitive touchscreen (d).

ABSTRACT
Embedding sensors into objects allow them to recognize various interactions. But, sensing usually requires active electronics that are often costly, need time to be assembled, and constantly draw power. Thus, we propose *off-line sensing*: passive 3D-printed sensors that detect one-time interactions, such as accelerating or flipping, but neither require active electronics nor power at the time of the interaction. They memorize a pre-defined interaction via an embedded structure filled with a conductive medium (e.g., a liquid). Whether a sensor was exposed to the interaction can be read-out via a capacitive touchscreen. Sensors are printed in a single pass on a consumer-level 3D printer. Through a series of experiments, we show the feasibility of off-line sensing.

Author Keywords
3D printing; digital fabrication; capacitive sensing; metamaterial; mechanism; input; sensors;

ACM Classification Keywords
H.5.2 Information Interfaces and Presentation: User Interfaces – Input devices and strategies.

INTRODUCTION
With the advances in 3D printing, research is emerging to support users in rapidly fabricating personalized objects [15, 16, 17, 27] and in adding interactive functionality by attaching electronics [6, 13, 19, 20] or creating internal structures [1, 10, 21, 30, 24]. While embedding functionality directly into the objects, they often require to attach and power electronics which quickly gets laborious and costly when dealing with many objects or long deployment timespans. To overcome this issue, we believe that encoding functionality within the object's 3D structure is a promising approach to make objects interactive without the need for power-consuming electronics.

We contribute 3D-printed structures, called *off-line sensors*, that detect one-time interactions performed with objects without requiring any active electronics nor power during the interaction. Off-line sensors respond to load, pressure, acceleration, tilt, flip, and rising or falling temperature. They consist of conductive and insulating solids combined with chambers containing a medium, such as a conductive liquid (cf. [23]). The sensor's properties (e.g., on how much load it reacts) can be defined before printing via a specification UI. Then, the sensor is 3D-printed, post-processed and deployed into an interaction context. Users extract whether the sensor was exposed to the interaction by using a capacitive touchscreen. Based on capacitive coupling [18, 24], off-line sensors intentionally alter their response on the touchscreen depending on whether a capacitive path between the conductive solid and the medium is formed. Off-line sensors can be attached to or fabricated into objects to monitor their status (e.g., to assure proper handling of a tool) or check environmental conditions (e.g., a freeze-aware outdoor plant pot). As depicted in Figure 1, an off-line sensor may be used to ensure a parcel's proper handling.

We believe that off-line sensing is not a competing but complementing approach compared to traditional sensing, suited for sensor deployments without supervision, possibly over a long timespan. To that end, we aim to take a first step in exploring off-line sensing for HCI by addressing fundamental conceptual and technical challenges. We focus on a basic, yet widely used set of interactions that serve as a foundation for more advanced interactions. Even though off-line sensing is not tied to 3D printing, we intend to contribute to the vision of interactive objects that are individually designed and printed on-demand based on application scenarios or user's needs [30].

CHI 2018, April 21–26, 2018, Montréal, QC, Canada

ACM 978-1-4503-5620-6/18/04…$15.00.
DOI: https://doi.org/10.1145/3173574.3173756

The main contributions of this paper are:

- A consumer-level fabrication pipeline to easily create, 3D-print and capacitively read-out off-line sensors.
- Off-line sensors that memorize load, pressure, acceleration, tilt, flip over, and rising or falling temperature.
- A proof-of-concept evaluation showing their feasibility.

RELATED WORK

This paper is situated in the areas of metamaterials and digital fabrication of interactive objects.

Metamaterials

Metamaterials, i.e., structures engineered to yield new properties, are investigated in material science to indicate, for instance, tilting or shock (cf. [26]). Also, an emerging stream of research investigates how to digitally fabricate objects containing metamaterials. Such metamaterials convey digital information by means of terahertz imaging [31], magnetic storage [11], or air pockets [14]. Moreover, they are used to enrich fabricated objects with mechanical functionality [8], logical operations [9], or self-folding [25]. Adding to this stream of research, off-line sensors allow objects to memorize one-time interactions that can be integrated into 3D-printed objects and digitally read-out with a standard capacitive touchscreen.

Fabricating Interactive 3D Objects

Another stream of research investigates how to print or embed customized interactive sensors into objects. This includes adding interactive input and output functionalities in 3D-printed objects through light pipes [1, 30], by filling internal pipes with media post-print [21], or via pipes that transmit sound [13]. Other approaches 3D-print interactive objects by means of conductive spray [10, 17], conductive plastic [2, 12, 22, 24], conductive threads [7] or pneumatics [28]. Adding to this body of research, off-line sensors are 3D-printed in a single pass without requiring additional assembly of electronics.

OFF-LINE FABRICATION PIPELINE

This section introduces the off-line sensing principle underlying all off-line sensors and the fabrication pipeline to easily create them, starting from the specification of a sensor to extracting whether it was exposed to an interaction.

Off-Line Sensing Principle

Off-line sensors consist of conductive electrodes, insulating material and hollow volumes, called *chambers*, filled with a conductive medium (e.g., tap water). They employ two types of electrodes (see Figure 2a):

- The *user electrode* connects the user's finger to the sensor and thus grounds it with respect to the touchscreen.
- The *touchscreen electrode* connects the sensor to the underlying capacitive touchscreen and enables it to extract the sensor's state.

As depicted in Figure 2b, the sensor's internal state is extracted via the touchscreen electrode as follows: Once a conductive medium alters the electrical properties of the sensor, a capacitive path from the user's finger throughout the sensor onto the touchscreen is formed. This results in a measurable change in capacitance at the touchscreen.

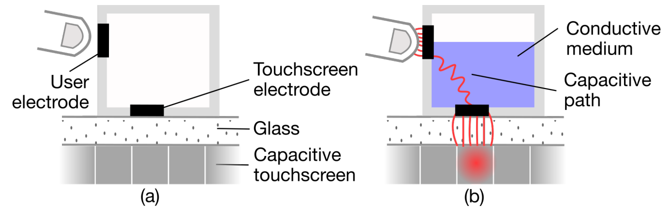

Figure 2. Sensing principle: Depending on the sensor's state, a conductive path between the user and the touchscreen is formed (b) or not (a).

Specification

A specification UI enables users to choose from a list of off-line sensors (see Figure 1a). The UI eases the creation of a sensor by removing the need to be an expert in CAD. It provides information on each sensor and allows the user to adjust properties depending on the sensor (e,g., the load or pressure to be sensed), the 3D printer, and the touchscreen (e.g., the electrode's size, an important factor depending on the printer's precision and touchscreen). After the sensor's model is created, the UI offers the user to export:

- 3D-printable files for conductive and insulating materials
- Instructions on how to post-process the sensor
- A definition file stating the location of electrodes, a capacitive marker for identification, and the sensor's properties

Printing and Post-Processing

The user slices the 3D-printable files with printer-specific settings and hands it over to the 3D printer (see Figure 1b). After 3D printing, the sensor must be further prepared for deployment by following the generated instructions. For most sensors, only filling with a conductive medium (e.g., tap water) is required. Some sensors require further post-processing, such as freezing or cutting off specific parts.

Deployment and Interaction

After post-processing, the user deploys the sensor in the desired interaction context (see Figure 1c). If the sensor was exposed to the pre-defined interaction, its state is permanently altered. Otherwise, it remains in its initial state.

Collection and Extraction

For the user to check whether an interaction occurred, she uses an Android app on her mobile device (see Figure 1d). While connecting her finger to the user electrode, she places the sensor on a highlighted area on the touchscreen.

The application then detects the sensor through a conductive marker on its bottom (cf. [3, 24, 29]) and extracts whether the interaction occurred by analyzing if a touch point exists at a pre-defined location, saved together with the marker's id in the definition file during specification.

OFF-LINE SENSORS

In the following, we present specific off-line sensors, i.e., 3D-printed structures that employ off-line sensing. As illustrated in Figure 3, we focus on a set of interactions that concern:

- Mechanical forces: load (a) or pressure (b) on an object
- Physical manipulations: acceleration (c), tilt (d), or flip (e)
- Environmental conditions: rising (f) or falling (g) temperature around an object

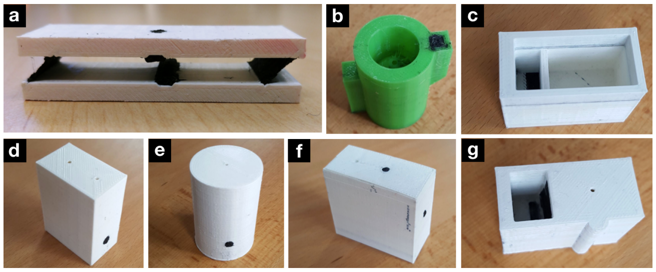

Figure 3. Overview of off-line sensors that detect load (a), pressure (b), acceleration (c), tilt (d), flip (e), rising (f), and falling (g) temperature.

Loading

This sensor reacts to an evenly distributed load force caused, for instance, by applying a certain weight. It consists of two plates on top of each other, connected by two to six thin pillars (see Figure 4). The pillars have an angle of 45° to facilitate a controlled buckling. Both plates also contain a user electrode on top and a touchscreen electrode at the bottom. If the load limit has not yet been exceeded, the two electrodes are a few millimeters apart. If a big enough load is evenly applied, the pillars break. As a result, the user and touchscreen electrode connect to each other. This creates a direct connection between the finger and the touchscreen during the read-out process. In order to improve the connection between both electrodes, they are slightly offset to one side, since a slight displacement of the upper plate occurs during the buckling.

Practical Challenges

After printing, the sensor must be checked for unwanted connections between the electrodes. These can be caused by oozing effects of the printing material, which falsifies the response. During deployment, the sensor only changes its state when the applied force is perpendicular to the plates, as the pillars are designed to only break that way. In other cases, the sensor's state will not change. To simultaneously check for loads applied in other directions, multiple copies of this sensors may be printed and oriented as such.

For read-out, the bottom plate of the sensor is placed on the touchscreen. Depending on the printer, the electrode should be slightly displaced outwards to improve the touchscreen's connection. As the finger is softer and, thus, better connects to the electrode, this is not required for the user electrode. Also, a slight force on the sensor should be exerted in order to counteract a possible spring effect of the pillars.

Pressing

The pressing sensor changes its state when squeezed with a certain pressure. The sensor consists of two superimposed cone-shaped chambers (see Figure 5): The lower chamber is

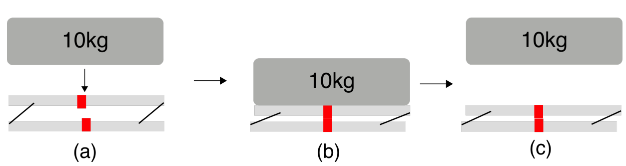

Figure 4. Once a weight is applied (b), the previously unconnected electrodes (a) connect (c). Both electrodes are shown in red.

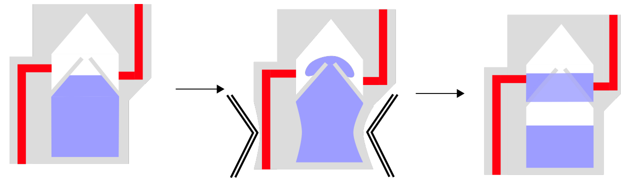

Figure 5. By applying pressure, the flexible material is compressed and liquid is poured out of the upper hole.

filled with liquid. The upper chamber contains both electrodes. Both chambers are connected by a small hole at the top of the lower chamber's cone. If the sensor is squeezed, the lower chamber is compressed and the liquid is pressed through the hole, separating both chambers. The liquid is collected in the upper chamber and connects the two electrodes.

Practical Challenges

This sensor should be printed with flexible material to allow for compression. To avoid filling the upper chamber with liquid, a syringe with a needle should be used.

Accelerating

The acceleration sensor reacts to accelerations that exceed a pre-defined level. It consists of two chambers (see Figure 6). The larger one is filled with a conductive liquid (e.g., tap water). Both chambers are separated by a wall that is variable in height. If the sensor is accelerated in the opposite direction of the smaller chamber, the liquid inside the chamber is forced into the direction of the smaller chamber because of the inertia. If the acceleration is large enough, the liquid spills over the parting wall and is caught in the smaller chamber. For read-out, the smaller chamber contains a user electrode and a touchscreen electrode, only connected by a liquid in case of acceleration. For instance, the amount of liquid and the height of the wall can be varied to alter the acceleration level.

Practical Challenges

The larger chamber must be filled with a liquid either during printing or afterward. During deployment, users must ensure that the sensor is not tilted. A small angular change can already significantly alter the acceleration limit. Ideally, the sensor is oriented horizontally without tilt. For read-out, the sensor is placed on the touchscreen and touched with a finger. During this phase, small tilts are irrelevant, while greater tilts can lead to a falsification of the state.

Tilting

Using this sensor, tilts around 90°, depending on the liquid's volume, can be detected. The sensor consists of two chambers (see Figure 7): The left chamber contains a liquid. If the sensor is tilted (i.e., the left chamber is above the right), the liquid flows through the hole down and connects the electrodes.

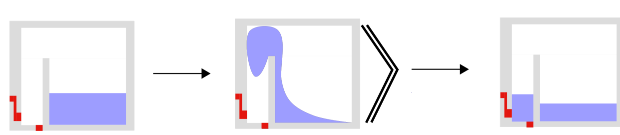

Figure 6. By accelerating, liquid spills over into the second chamber.

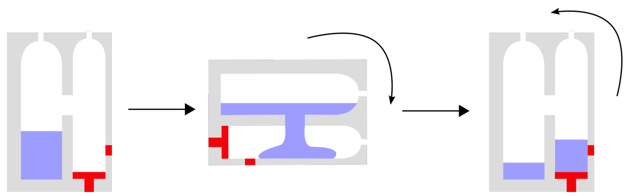

Figure 7. By tilting, the liquid is disposed in the second chamber.

Practical Challenges

If the chamber's volume is too small compared to the connecting hole, there are often problems with air displacement. To compensate, both chambers either require a hole for air leakage or the size of the connecting hole needs to be increased. The tilt angle can be influenced best by varying the amount of liquid. Using less liquid, the tilt angle ranges around 90°. Using more liquid, even smaller tilt angles are recognized.

Flipping Over

The flipping over sensor consists of two interlocked chambers (see Figure 8). The inner chamber is filled with liquid. If the sensor is flipped over, the liquid flows from the inner into the outer chamber. When rotated by only 90°, the liquid remains through the dome-shaped cover in the inner chamber.

Practical Challenges

After printing, a liquid needs to be filled only into the inner chamber. To avoid filling the outer chamber, a syringe with a needle should be used. If too much liquid is used, the inner chamber will overflow, which falsifies the sensor's response.

Rising Temperature

This sensor detects temperature changes that rise above a certain limit through thermal conduction (cf. Fourier's law). If the sensor is kept below a certain temperature during deployment, the state will not change. But, if the temperature is increased above the limit, the state change will occur. Its state is also altered if the threshold was only temporarily exceeded.

As illustrated in Figure 9, the sensor is subdivided into two chambers. The smaller chamber is filled with a liquid (a). The two electrodes for the detection of the state are printed in the bigger chamber. If the sensor is stored under the liquid's melting point during deployment (b), the frozen liquid will remain in its form, and no liquid will enter the bigger chamber (c). However, if the sensor is stored above the melting point, the frozen liquid starts to melt, causing liquid to accumulate at the bottom of the smaller chamber (d). From there, it flows through a small tube into the adjacent bigger chamber, where it is then recognized by the presence of a connection between the

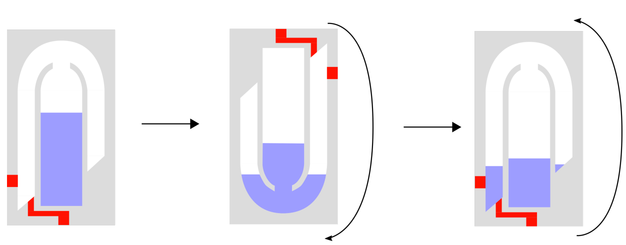

Figure 8. Flipping over the sensor results in a deposition of liquid into the second chamber.

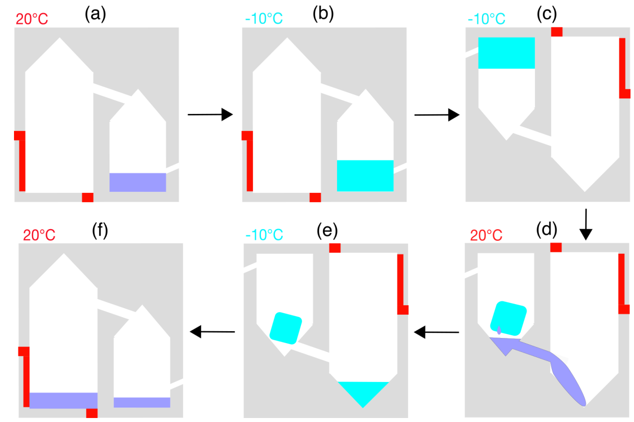

Figure 9. After filled (a) and frozen (b), the frozen liquid remains in the smaller chamber as long as the temperature is under a certain threshold (c). If the temperature rises, it is disposed into the bigger chamber (d/e) for later read-out (f).

electrodes. If the sensor is stored again under the melting point before read-out (e), the liquid freezes in the bigger chamber. However, as the liquid remains in this chamber until read-out, the state change can still be detected by heating the sensor (f).

Practical Challenges

To prepare for deployment, the liquid must be filled through a small hole. To that end, the sensor must be placed upside down (see Figure 9a), because otherwise the liquid immediately flows into the next chamber. After this step, the object (i.e., the liquid) is frozen and then turned around again for deployment.

If the state is to be read-out after deployment, the sensor must be rotated upside down again, so that the touchscreen electrode points downwards. In this orientation, the rotation prevents the ice, which is still present in the chamber, from flowing into the other chamber. Since ice is not electrically conductive, it must be melted before read-out.

Falling Temperature

The falling temperature sensor changes its state when stored for a certain time under a temperature limit. The sensor consists of two chambers (see Figure 10). The larger of the two chambers is completely filled with a conductive liquid with negative thermal expansion (i.e., it increases in volume when cooled). The smaller one contains both electrodes. Both chambers are liquid-tightly separated from each other by a thin wall. When the liquid freezes, it increases in volume and breaks through the thin wall. As a result, the wall is no longer leak proof. If the frozen liquid is heated again, it leaks through the crack into the second chamber and connects the electrodes.

Practical Challenges

As this sensor requires a liquid with negative thermal expansion, we employed tap water (it expand in volume approx. 9%). After printing, the larger chamber must be completely

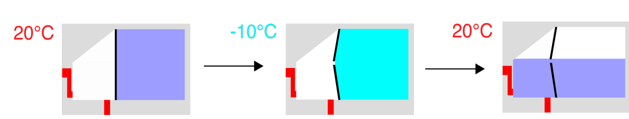

Figure 10. Due to the increased volume of a frozen liquid (middle), a slim wall breaks, resulting in the deposition of liquid into the left chamber.

filled with liquid. The sensor can be read-out if not frozen, as then enough liquid is able to connect the electrodes.

IMPLEMENTATION

The specification UI utilizes OpenSCAD scripts to create off-line sensors. As a consequence, sensors can be easily changed or added by providing a new OpenSCAD script.

For printing, we utilized the dual extrusion printer BCN3D Sigma to print conductive and insulating materials simultaneously. The accompanying software BCN3D Cura was used for slicing. The conductive electrodes consist of carbon-doped Proto-pasta Conductive PLA (cPLA) with a volume resistivity of 30–115 Ωcm (printing temperature of 220 °C at a cost of 140 €/kg). For insulating parts, Verbatim PLA was used (printing temperature of 212 °C at a cost of 30 €/kg). For the pressure sensor, NinjaFlex TPU was used (printing temperature of 225 °C at a cost of 90 €/kg).

Since in most cases the sensor can only be used once, less importance was placed on the printing quality. The thickness of the layers was set to 0.2 mm to keep the printing duration low. Retraction of the filament was enabled to prevent unwanted connections between the conductive parts. For all sensors, an infill density of 20% was chosen, which is adequate for sensors using normal PLA. Also, this density allows for sufficient flexibility in sensors made of flexible TPU. The printing speed was set to 40 mm/s for most sensors. Only for flexible TPU, the printing speed was reduced at the beginning of the print to ensure a better cohesion between the first few layers. Since sensors are filled with liquid in many cases, they were printed with a material flow of 110% for solid parts and 125% for flexible parts to avoid for leaking.

TECHNICAL EXPERIMENTS AND GUIDELINES

We conducted technical experiments to evaluate our prototypes of all off-line sensors. We report our findings and provide guidelines for designing and printing off-line sensors.

Loading

Our prototype of the load sensor has dimensions of 6.1 cm $\times$ 2 cm $\times$ 1.4 cm. After triggering, the sensor's height is reduced to 1.1 cm. The maximal load depends on several factors which may be varied by designers:

- the number and thickness of pillars
- the pillar's material strength and angle
- the printing direction and inter-layer adhesion strength

As the sensor is designed for evenly distributed loads, the effect of the pillars' distribution on the maximal load is almost negligible. However, varying levels of load can still be recognized by controlling the number of pillars. Thus, we evaluated the load sensor with 2, 4, and 6 pillars (thickness 0.5 mm) and increased the weight until it responded. We found that three levels of loads can be reliably distinguished: The sensor reacts for 2 pillars at 5.2 kg, for 4 pillars at 10.5 kg, and for 6 pillars at 16.4 kg. Using more pillars is easily possible but requires a bigger size of the overall sensor. Moreover, we tested normal PLA for the pillars. However, due to the elastic material properties of PLA, the electrodes rebound despite the sensor was triggered. This can be counteracted by applying more pressure from the finger during read-out. However, the amount required was unpleasant, both for the finger and for the stability of the touchscreen. Thus, we decided to use cPLA for the pillars, as it is more brittle than normal PLA. As a result, the sensor does not rebound anymore. Both plates should be printed in sideways direction to improve the quality of the pillars and to reduce the risk that the sensor peels off the printing plate during printing. To that end, the base area also has been enlarged.

Pressing

Our prototype of the pressing sensor has a diameter of 3.5 cm (height of 2.6 cm). The sensor's reaction depends on several factors which may be varied by designers:

- the liquid's volume
- the insulating material's infill density

We found that 5 ml of tap water results in a reliable detection of pressure. The amount of pressure required can be fine-tuned by varying the infill density or by changing the amount of liquid. Also, the printing quality is an important factor as otherwise the flexible TPU leaks liquid. We found that sensors should be printed with a slower printing speed of 30 mm/s and an increased material flow of 125%.

Accelerating

Our prototype of the accelerating sensor has dimensions of 4 cm $\times$ 2.4 cm $\times$ 4 cm. The sensor's reaction depends on several factors which may be varied by designers:

- the wall height and dimension of the chamber
- the liquid's viscosity and volume
- the angle of acceleration

We measured at which acceleration the state changed for varying wall heights and 3 ml of tap water. We mounted the sensor to a smartphone and used its sensors to compare the acceleration to the sensor's response. By repeating different levels of acceleration (between 1-15 m/s^2) 20 times, we found that for our prototype at least two accelerations can be reliably distinguished: For a wall height of 10 mm, 5 m/s^2 (SD 1 m/s^2) acceleration was detected (e.g., equals a starting car). For a wall height of 18 mm, 12 m/s^2 (SD 1 m/s^2) acceleration was detected (e.g., equals an emergency stop in a car). By further varying factors (e.g., viscosity), more levels of acceleration could be distinguished.

Tilting

Our prototype of the tilting sensor has dimensions of 2.8 cm $\times$ 1.8 cm $\times$ 4 cm. The sensor's reaction depends on several factors which may be varied by designers:

- the liquid's viscosity
- the amount of liquid

We found that using 2 ml of tap water is sufficient to operate this sensor. However, the main challenge is that chambers should not be airtightly closed because otherwise, the remaining air in both chambers blocks the liquid from flowing into the second chamber. Thus, we used two air-holes at the top of the sensor to allow for a sufficient air circulation.

Flipping Over
Our prototype of the flipping over sensor has a diameter of 3.4 cm (height of 5.1 cm). The sensor's reaction depends on the same factors as for tilting. Also, similar to tilting, air circulation is a challenge if the sensor is airtightly closed. As an air-hole at the top would result in leaking liquid in the case of flipping over, we increased the size of the hole connecting both chambers. Thereby, air and liquid can be exchanged between chambers more easily.

Rising Temperature
Our prototype of the rising temperature sensor has dimensions of 4.4 cm $\times$ 2 cm $\times$ 3 cm. We evaluated tap water (melting point approx. 0 °C) and 2 mm PLA walls (with rather low thermal conductivity). The defrosting time depends on several factors which may be varied by designers:
- the temperature difference between inside and outside
- the time of exposure to the temperature difference
- the insulating material's thermal conductivity and thickness

By varying the factors of Fourier's law (e.g., other materials or liquids with other melting points), the defrosting time (i.e., the sensor's response temperature) can be controlled.

Falling Temperature
Our prototype for the falling temperature sensor has dimensions of 4.3 cm $\times$ 2.2 cm $\times$ 3.2 cm. Besides the factors for rising temperature, the freezing time depends on these factors:
- the inner wall's material strength and thickness
- the liquid's initial volume

As this sensor is based on a fracture in its internal structure, it highly depends on the inner wall's material properties. If the printing quality is too high, it will not break. Thus, as for loading, we used the brittler cPLA. By freezing the sensor 20 times, we found that an inner wall thickness of 0.5 mm results in a reliable fracture to trigger the state change. Similar to the previous sensor, the reaction temperature can be controlled by using liquids with varying freezing points or changing the freezing temperature of tap water by adding salt.

DISCUSSION AND LIMITATIONS
This paper presents first results on off-line sensors that memorize interactions by leveraging capacitive coupling. However, our approach has limitations that must be considered during design, printing, and sensing.

Manual Post-Processing
Currently, off-line sensors need to be manually post-processed to remove support and add a conductive medium (e.g., using a syringe). However, the deposition of liquids into sensors during 3D printing can be automated using a syringe extruder in combination with a pump (cf. [32]). Besides for loading, all off-line sensors are intentionally designed to be printable without support material. With the emergence of multi-extruder printers, support may be printed with water-soluble PVA and washed out after printing.

Reversibility and Reusability
Off-line sensors operate only once for a pre-defined interaction. They are intentionally designed to withstand accidental or malicious attempts to reverse their state (e.g., by using conic funnels or small holes). Yet, sensors that use a liquid may be completely dried and refilled several times, as the solid structures are unmodified. However, even small residues of liquid are sufficient to trigger a sensor, which is hard to reverse due to adhesion. Alternatively, sensors may be either disposed, as it mostly consist of biodegradable PLA, or recycled as 3D printing filament (e.g., via a filament extruder [5]).

Continuity
Despite off-line sensors respond well to one discrete interaction, they are unable to sense an interaction performed multiple times. Moreover, we focus on binary measurements with standard touchscreens to strengthen practicability. While different discrete levels can be detected simultaneously by printing multiple sensors with varying properties, future work could advance the detection towards continuous levels of an interaction in one single sensor by correlating liquid levels inside a chamber with capacitive raw data provided by the touchscreen.

Scalability
Scalability is an important issue, as the size of a sensor and of the capacitive touchscreen may vary from small to very large. The sensors' electrodes presented in this paper are optimized for the size of a fingertip (16–20 mm [4]). Also, the approach requires a volumetric object inside which a sensor can be inserted and conductors can be routed. Thus, geometries with thin structures, high curvatures, or cavities remain challenging.

The minimal size of a sensor is limited by the resolution and the nozzle diameter of today's commodity 3D printers. Using our print setup, the minimal cross-sectional size of an electrodes' conductor is 3x3 mm². The second limit to miniaturizing sensors relates to the volume of a chamber. If shrunk too much, it may not be sufficient to hold enough liquid anymore.

Combination of Sensors
Off-line sensors may be combined into one 3D-printed object by merging and printing multiple sensors together. However, sensors based on different conductive media may not be compatible (e.g., frozen vs. liquid media). Also, environmental conditions need to be considered. For instance, using a liquid to detect flipping over in a refrigerated car remains challenging as the freezing point of the liquid needs to be sufficiently low.

CONCLUSION AND FUTURE WORK
This paper has presented *off-line sensing*: a set of sensors that memorize pre-defined interaction via embedded 3D-printed structures filled with a conductive medium. Using off-line sensing, we contribute a variety of off-line sensors that sense load, pressure, acceleration, tilt, flip over, and temperature. Whether an object was exposed to the interaction can be readout via placing it on a standard capacitive touchscreen. Using a consumer-level fabrication pipeline, off-line sensors can be easily created, printed and used. Future work should address more advanced (e.g., continuous) interactions and further applications, where it is beneficial to deploy off-line sensors.

ACKNOWLEDGMENTS
We thank Florian Müller and Florian Krause for their support and the reviewers for their valuable comments.

REFERENCES

1. Eric Brockmeyer, Ivan Poupyrev, and Scott Hudson. 2013. PAPILLON: Designing Curved Display Surfaces with Printed Optics. In *Proceedings of the 26th annual ACM symposium on User interface software and technology - UIST '13*. ACM Press, New York, New York, USA, 457–462. DOI: http://dx.doi.org/10.1145/2501988.2502027
2. Jesse Burstyn, Nicholas Fellion, and Paul Strohmeier. 2015. *PrintPut: Resistive and Capacitive Input Widgets for Interactive 3D Prints*. Lecture Notes in Computer Science, Vol. 9296. Springer International Publishing, Cham. 332–339 pages. DOI: http://dx.doi.org/10.1007/978-3-319-22701-6
3. Liwei Chan, Stefanie Müller, Anne Roudaut, and Patrick Baudisch. 2012. CapStones and ZebraWidgets: Sensing Stacks of Building Blocks, Dials and Sliders on Capacitive Touch Screens. In *Proceedings of the 2012 ACM annual conference on Human Factors in Computing Systems - CHI '12*. ACM Press, New York, New York, USA, 2189. DOI: http://dx.doi.org/10.1145/2207676.2208371
4. Kiran Dandekar, Balasundar I Raju, and Mandayam a Srinivasan. 2003. 3-D Finite-Element Models of Human and Monkey Fingertips to Investigate the Mechanics of Tactile Sense. *Journal of Biomechanical Engineering* 125, 5 (2003), 682. DOI: http://dx.doi.org/10.1115/1.1613673
5. Filabot. 2018. Filabot EX2 Filament Extruder https://www.filabot.com. (2018). Last accessed: January 2018.
6. Jonathan Hook, Thomas Nappey, Steve Hodges, Peter Wright, and Patrick Olivier. 2014. Making 3D Printed Objects Interactive Using Wireless Accelerometers. In *Proceedings of the extended abstracts of the 32nd annual ACM conference on Human factors in computing systems - CHI EA '14*. ACM Press, New York, New York, USA, 1435–1440. DOI: http://dx.doi.org/10.1145/2559206.2581137
7. Scott E. Hudson. 2014. Printing Teddy Bears: A Technique for 3D Printing of Soft Interactive Objects. In *Proceedings of the 32nd annual ACM conference on Human factors in computing systems - CHI '14*. ACM Press, New York, New York, USA, 459–468. DOI: http://dx.doi.org/10.1145/2556288.2557338
8. Alexandra Ion, Johannes Frohnhofen, Ludwig Wall, Robert Kovacs, Mirela Alistar, Jack Lindsay, Pedro Lopes, Hsiang-ting Chen, and Patrick Baudisch. 2016. Metamaterial Mechanisms. In *Proceedings of the 29th Annual Symposium on User Interface Software and Technology - UIST '16*. ACM Press, New York, New York, USA, 529–539. DOI: http://dx.doi.org/10.1145/2984511.2984540
9. Alexandra Ion, Ludwig Wall, Robert Kovacs, and Patrick Baudisch. 2017. Digital Mechanical Metamaterials. In *Proceedings of the 2017 CHI Conference on Human Factors in Computing Systems - CHI '17*. ACM Press, New York, New York, USA, 977–988. DOI: http://dx.doi.org/10.1145/3025453.3025624
10. Yoshio Ishiguro and Ivan Poupyrev. 2014. 3D Printed Interactive Speakers. In *Proceedings of the 32nd annual ACM conference on Human factors in computing systems - CHI '14*. ACM Press, New York, New York, USA, 1733–1742. DOI: http://dx.doi.org/10.1145/2556288.2557046
11. Vikram Iyer, Justin Chan, and Shyamnath Gollakota. 2017. 3D Printing Wireless Connected Objects. *ACM Transactions on Graphics* 36, 6 (nov 2017), 1–13. DOI: http://dx.doi.org/10.1145/3130800.3130822
12. Kunihiro Kato and Homei Miyashita. 2016. 3D Printed Physical Interfaces that can Extend Touch Devices. In *Proceedings of the 29th Annual Symposium on User Interface Software and Technology - UIST '16 Adjunct*. ACM Press, New York, New York, USA, 47–49. DOI: http://dx.doi.org/10.1145/2984751.2985700
13. Gierad Laput, Eric Brockmeyer, Scott E. Hudson, and Chris Harrison. 2015. Acoustruments: Passive, Acoustically-Driven, Interactive Controls for Handheld Devices. In *Proceedings of the 33rd Annual ACM Conference on Human Factors in Computing Systems - CHI '15*. ACM Press, New York, New York, USA, 2161–2170. DOI: http://dx.doi.org/10.1145/2702123.2702414
14. Dingzeyu Li, Avinash S Nair, Shree K Nayar, and Changxi Zheng. 2017. AirCode: Unobtrusive Physical Tags for Digital Fabrication Dingzeyu. In *Proceedings of the 30th Annual ACM Symposium on User Interface Software and Technology - UIST '17*. ACM Press, New York, New York, USA, 449–460. DOI: http://dx.doi.org/10.1145/3126594.3126635
15. Stefanie Mueller, Sangha Im, Serafima Gurevich, Alexander Teibrich, Lisa Pfisterer, François Guimbretière, and Patrick Baudisch. 2014a. WirePrint: 3D Printed Previews for Fast Prototyping. In *Proceedings of the 27th annual ACM symposium on User interface software and technology - UIST '14*. ACM Press, New York, New York, USA, 273–280. DOI: http://dx.doi.org/10.1145/2642918.2647359
16. Stefanie Mueller, Tobias Mohr, Kerstin Guenther, Johannes Frohnhofen, Kai-Adrian Rollmann, and Patrick Baudisch. 2014b. faBrickation: Fast 3D Printing of Functional Objects by Integrating Construction Kit Building Blocks. In *Proceedings of the extended abstracts of the 32nd annual ACM conference on Human factors in computing systems - CHI EA '14*. ACM Press, New York, New York, USA, 527–530. DOI: http://dx.doi.org/10.1145/2559206.2574779
17. Huaishu Peng, Rundong Wu, Steve Marschner, and François Guimbretière. 2016. On-The-Fly Print: Incremental Printing While Modeling. In *Proceedings of the 2016 CHI Conference on Human Factors in Computing Systems - CHI '16*. ACM Press, New York, New York, USA, 887–896. DOI: http://dx.doi.org/10.1145/2858036.2858106

18. Jun Rekimoto. 2002. SmartSkin: An Infrastructure for Freehand Manipulation on Interactive Surfaces. In *Proceedings of the SIGCHI conference on Human factors in computing systems Changing our world, changing ourselves - CHI '02*. ACM Press, New York, New York, USA, 113. DOI:http://dx.doi.org/10.1145/503376.503397

19. Munehiko Sato, Ivan Poupyrev, and Chris Harrison. 2012. Touché: Enhancing Touch Interaction on Humans, Screens, Liquids, and Everyday Objects. In *Proceedings of the 2012 ACM annual conference on Human Factors in Computing Systems - CHI '12*. ACM Press, New York, New York, USA, 483. DOI: http://dx.doi.org/10.1145/2207676.2207743

20. Valkyrie Savage, Colin Chang, and Björn Hartmann. 2013. Sauron: Embedded Single-camera Sensing of Printed Physical User Interfaces. In *Proceedings of the 26th annual ACM symposium on User interface software and technology - UIST '13*. ACM Press, New York, New York, USA, 447–456. DOI: http://dx.doi.org/10.1145/2501988.2501992

21. Valkyrie Savage, Ryan Schmidt, Tovi Grossman, George Fitzmaurice, and Björn Hartmann. 2014. A Series of Tubes: Adding Interactivity to 3D Prints Using Internal Pipes. In *Proceedings of the 27th annual ACM symposium on User interface software and technology - UIST '14*. ACM Press, New York, New York, USA, 3–12. DOI:http://dx.doi.org/10.1145/2642918.2647374

22. Martin Schmitz, Mohammadreza Khalilbeigi, Matthias Balwierz, Roman Lissermann, Max Mühlhäuser, and Jürgen Steimle. 2015. Capricate: A Fabrication Pipeline to Design and 3D Print Capacitive Touch Sensors for Interactive Objects. In *Proceedings of the 28th Annual ACM Symposium on User Interface Software & Technology - UIST '15*. ACM Press, New York, New York, USA, 253–258. DOI: http://dx.doi.org/10.1145/2807442.2807503

23. Martin Schmitz, Andreas Leister, Niloofar Dezfuli, Jan Riemann, Florian Müller, and Max Mühlhäuser. 2016. Liquido: Embedding Liquids into 3D Printed Objects to Sense Tilting and Motion. In *Proceedings of the 2016 CHI Conference Extended Abstracts on Human Factors in Computing Systems - CHI EA '16*. ACM Press, New York, New York, USA, 2688–2696. DOI: http://dx.doi.org/10.1145/2851581.2892275

24. Martin Schmitz, Jürgen Steimle, Jochen Huber, Niloofar Dezfuli, and Max Mühlhäuser. 2017. Flexibles: Deformation-Aware 3D-Printed Tangibles for Capacitive Touchscreens. In *Proceedings of the 2017 CHI Conference on Human Factors in Computing Systems - CHI '17 (CHI '17)*. ACM Press, New York, New York, USA, 1001–1014. DOI: http://dx.doi.org/10.1145/3025453.3025663

25. Subramanian Sundaram, David S Kim, Marc A Baldo, Ryan C Hayward, and Wojciech Matusik. 2017. 3D-Printed Self-Folding Electronics. *ACS Applied Materials & Interfaces* 9, 37 (sep 2017), 32290–32298. DOI:http://dx.doi.org/10.1021/acsami.7b10443

26. Uline. 2018. Damage Indicators https://www.uline.com/Grp_332/Damage-Indicators. (2018). Last accessed: Januar 2018.

27. Udayan Umapathi, Hsiang-Ting Chen, Stefanie Mueller, Ludwig Wall, Anna Seufert, and Patrick Baudisch. 2015. LaserStacker: Fabricating 3D Objects by Laser Cutting and Welding. In *Proceedings of the 28th Annual ACM Symposium on User Interface Software & Technology - UIST '15*. ACM Press, New York, New York, USA, 575–582. DOI: http://dx.doi.org/10.1145/2807442.2807512

28. Marynel Vázquez, Eric Brockmeyer, Ruta Desai, Chris Harrison, and Scott E. Hudson. 2015. 3D Printing Pneumatic Device Controls with Variable Activation Force Capabilities. In *Proceedings of the 33rd Annual ACM Conference on Human Factors in Computing Systems - CHI '15*. ACM Press, New York, New York, USA, 1295–1304. DOI: http://dx.doi.org/10.1145/2702123.2702569

29. Simon Voelker, Kosuke Nakajima, Christian Thoresen, Yuichi Itoh, Kjell Ivar Øvergrd, and Jan Borchers. 2013. PUCs: Detecting Transparent, Passive Untouched Capacitive Widgets on Unmodified Multi-touch Displays. In *Proceedings of the 2013 ACM international conference on Interactive tabletops and surfaces - ITS '13*. ACM Press, New York, New York, USA, 101–104. DOI: http://dx.doi.org/10.1145/2512349.2512791

30. Karl Willis, Eric Brockmeyer, Scott Hudson, and Ivan Poupyrev. 2012. Printed Optics: 3D Printing of Embedded Optical Elements for Interactive Devices. In *Proceedings of the 25th annual ACM symposium on User interface software and technology - UIST '12*. ACM Press, New York, New York, USA, 589. DOI: http://dx.doi.org/10.1145/2380116.2380190

31. Karl D. D. Willis and Andrew D. Wilson. 2013. InfraStructs: Fabricating Information Inside Physical Objects for Imaging in the Terahertz Region. *ACM Transactions on Graphics* 32, 4 (jul 2013), 138:1–138:10. DOI:http://dx.doi.org/10.1145/2461912.2461936

32. Jonas Zehnder, Espen Knoop, Moritz Bächer, and Bernhard Thomaszewski. 2017. MetaSilicone: Design and Fabrication of Composite Silicone with Desired Mechanical Properties. *ACM Transactions on Graphics* 36, 6 (nov 2017), 1–13. DOI: http://dx.doi.org/10.1145/3130800.3130881